# Fragmentation Is Crucial for the Steady-State Dynamics of Actin Filaments

Kurt M. Schmoller,[†] Thomas Niedermayer,[‡] Carla Zensen,[†] Christine Wurm,[†] and Andreas R. Bausch[†*]
[†]Lehrstuhl für Biophysik E27, Technische Universität München, Garching, Germany; and [‡]Department of Theory and Bio-Systems, Max Planck Institute of Colloids and Interfaces, Potsdam, Germany

ABSTRACT Despite the recognition that actin filaments are important for numerous cellular processes, and decades of investigation, the dynamics of in vitro actin filaments are still not completely understood. Here, we follow the time evolution of the length distribution of labeled actin reporter filaments in an unlabeled F-actin solution via fluorescence microscopy. Whereas treadmilling and diffusive length fluctuations cannot account for the observed dynamics, our results suggest that at low salt conditions, spontaneous fragmentation is crucial.

## INTRODUCTION

The dynamics of actin filaments play a crucial role in many cellular processes, including cell motility and cell division (1). In vivo, treadmilling of actin filaments (i.e., an ATP-driven continuous lengthening at one end of the filament that is balanced by a shortening at the other end) is used by cells for force generation. In in vitro experiments, investigators have reconstituted actin-turnover-driven movement of bacteria or beads using actin and various actin-binding proteins (2,3). The underlying process—steady-state treadmilling of pure actin filaments—was first suggested more than 30 years ago (4). Measurements of the relevant association and dissociation rates at both filament ends have been used to estimate the turnover rate (4–6). Labeling of actin monomers with radioactive (7) or fluorescent dyes (8), and isotopic labeling (9,8) have provided direct evidence of an ATP-dependent exchange of actin monomers in polymerized steady-state actin. Additional information has been obtained by measuring the continuous phosphate release during steady state (10,11). Total internal reflection microscopy allows one to follow the polymerization and depolymerization of single actin filaments (12–15). Indeed, treadmilling of selected individual filaments has been observed (12). On the other hand, single-filament experiments revealed some puzzling features of actin dynamics, such as unexpectedly fast diffusive length fluctuations (12,13) and switching between different depolymerization rates (15,16). Our understanding of actin dynamics is additionally limited because ATP hydrolysis in actin filaments is still not completely understood (17), and only little is known about spontaneous fragmentation and annealing (18–21), although fragmentation has been suggested to be a crucial process for actin turnover in vivo (22).

Here, we show that a process that is dependent on the filament length plays a major role in the dynamics of a steady-state F-actin solution. The most probable candidate for this process is spontaneous fragmentation, which can be expected to show at least a linear dependence on the filament length. We investigated the time evolution of the length distribution of labeled actin reporter filaments in an unlabeled F-actin solution. The decay length of the exponential length distribution of visible filaments was found to decrease with time. Because treadmilling or diffusive length fluctuations cannot account for such behavior, we conclude that spontaneous fragmentation and annealing are major dynamic processes in pure actin solutions. Nevertheless, the determined ATPase activity indicates the presence of treadmilling dynamics, which influences the steady-state dynamics.

## MATERIALS AND METHODS

G-actin is obtained from rabbit skeletal muscle by a modified protocol of Spudich and Watt (23) as described previously (24). Polymerization is initiated by addition of a 10% volume of 10× polymerization buffer (pH 7.5; 20 mM Tris, 20 mM $MgCl_2$, 2 mM DTT, 5 mM ATP). $CaCl_2$ is added such that a final concentration of 0.2 mM is reached. For phosphate release measurements, lower concentrations of ATP are used such that including the ATP in the G-buffer, a total concentration of ≈175–290 $\mu$M ATP is obtained. Actin is labeled with the amine-reactive dye Alexa Fluor 555 carboxylic acid succinimidyl ester (A20009; Invitrogen, Darmstadt, Germany) or with Atto 488-NHS ester (41698; Sigma Aldrich, Taufkirchen, Germany) as previously described for Alexa Fluor 555 (24). A degree of labeling of ≈14–25% for Alexa Fluor 555 and ≈125% for Atto 488 is achieved. All experiments are performed at room temperature. Fluorescence microscopy data are acquired on a Zeiss (Jena, Germany) Axiovert 200 inverted microscope with a 100× oil immersion objective with a numerical aperture of 1.4. Two $\mu$L of the sample are pipetted onto a microscope slide and covered with a coverslip. Consequently, filaments are roughly oriented in the horizontal plane. Videos are taken above the lower surface with a frame rate of 10 or 30 Hz for covalently labeled actin and actin labeled with Alexa 488-phalloidin, respectively. To obtain length distributions, a gliding average of five images and a Gaussian blur are applied, background subtraction is done with ImageJ, and a threshold that is adjusted globally for the whole time series is used to create a binary image. Using the MATLAB R2007a function *regionprops* (The MathWorks, Natick, MA), interconnected objects with an area of >20 pixels are substituted by an ellipse that has the same normalized second central moments as the region, and the major axis length is used as a measure for filament length. Distributions are obtained from a minimum of 40 images and are

*Submitted April 11, 2011, and accepted for publication July 8, 2011.*

*Correspondence: abausch@ph.tum.de

Editor: Edward H. Egelman.



0006-3495/11/08/0803/6 $2.00

doi: 10.1016/j.bpj.2011.07.009

shown only for lengths > 20 pixels (3 $\mu$m). Qualitatively similar results are obtained if the number of pixels within an interconnected object is used as a measure for filament length. The EnzCheck phosphate assay (Invitrogen) (25) is used to monitor the release of inorganic phosphate by polymerized actin. To measure the phosphate release as a function of time, the desired number of samples equaling the number of data points in the time series are mixed contemporaneously and polymerized for 1 h. Then 0.2 mM of MESG substrate and a 1% volume of 100 U/ml stock solution PNP are added and incubated for 30 min. A spectrum is recorded at 24°C with a Lambda 25 spectrometer (PerkinElmer, Waltham, MA). The increase in absorbance at 360 nm as a function of time is translated to the phosphate release by using a calibration curve measured in the presence of F-actin.

## RESULTS AND DISCUSSION

Labeled and unlabeled actin filaments are polymerized separately for 3 h at a total actin concentration of 10 $\mu$M. To exclude dye-specific effects, experiments are performed with both Alexa Fluor 555- and Atto 488-labeled actin. As a first control, the length distribution of unlabeled actin filaments is measured after 3 h of polymerization and 50 h later by staining with labeled phalloidin directly before observation (Fig. 1). As expected from previous findings (26), an exponential length distribution is found at both points of time, which is best seen by computing the complementary cumulative length distribution. The decay length $\lambda_{\mathrm{all}}$ of the complementary cumulative distribution $D^{\mathrm{cum}}_{\mathrm{all}}(x) = \int_x^\infty D_{\mathrm{all}}(x')dx' = A^{\mathrm{cum}}_{\mathrm{all}} \cdot e^{-x/\lambda_{\mathrm{all}}}$ is equal to the decay length of the exponential length distribution $D_{\mathrm{all}}(x) = A_{\mathrm{all}} \cdot e^{-x/\lambda_{\mathrm{all}}}$. The prefactor is given by $A^{\mathrm{cum}}_{\mathrm{all}} = A_{\mathrm{all}} \cdot \lambda_{\mathrm{all}}$. Consistent with Sept et al. (20), the length distribution does not significantly change within 50 h (Fig. 1 *B*). This indicates that on the experimental timescale, all processes that affect the filament length distribution are balanced and a steady state is reached during the 3 h of polymerization.

In steady state, the growing of filaments by step-by-step association of monomers and annealing is balanced by the dissociation of protomers and spontaneous fragmentation. Thus, investigation of individual effects requires an experimental method that allows one to distinguish between the processes that cause filament growth and those that cause filament shrinkage. One such experiment involves mixing covalently labeled actin reporter filaments with an unlabeled F-actin solution and following the apparent length distribution of visible filaments over time via fluorescence microscopy. Whereas the overall length distribution of actin filaments is constant due to the steady state, spontaneous fragmentation, length fluctuations, and treadmilling cause shortening of the visible filaments. Processes that result in lengthening of the filaments are hidden in this approach because they are dominated by the incorporation of unlabeled monomers into the originally labeled filaments. Because spontaneous fragmentation, length fluctuations,

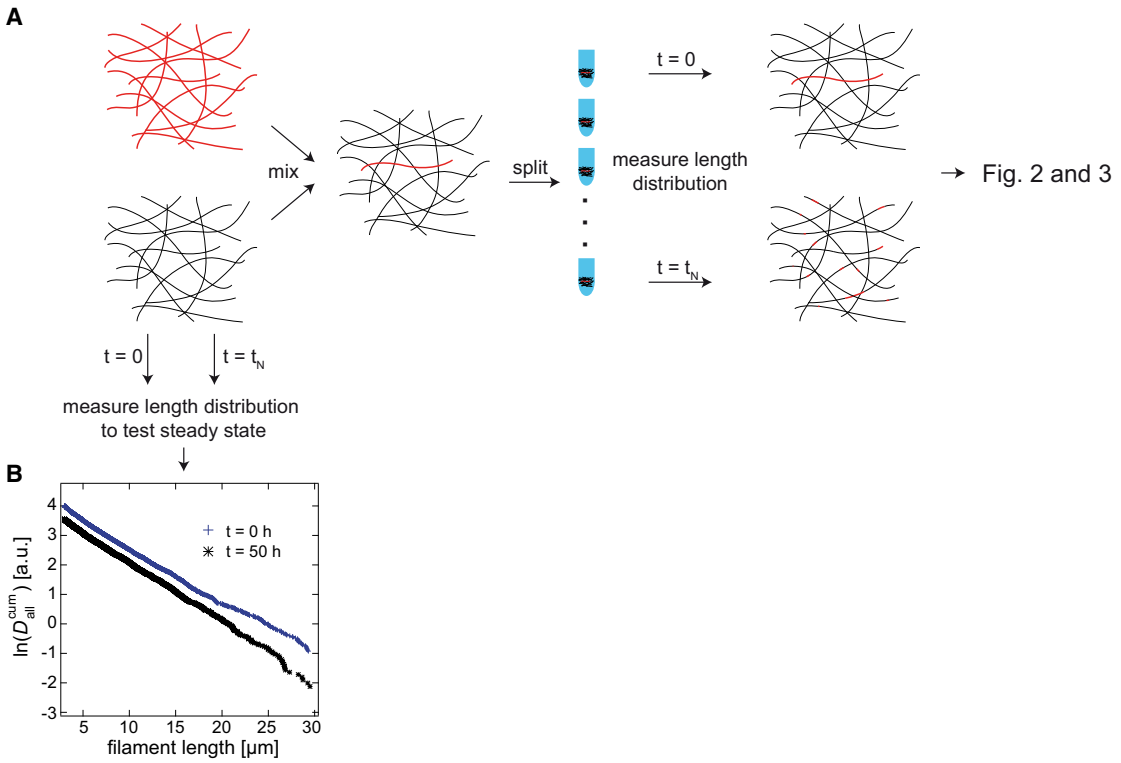


FIGURE 1 (*A*) Illustration of the experiment (data shown in Figs. 2 and 3). Labeled and unlabeled actin filaments are polymerized separately for 3 h at 10 $\mu$M. Labeled actin reporter filaments are mixed with a 300-fold excess of unlabeled F-actin. The sample is split each time and a new aliquot is used to measure the length distribution of labeled filament fragments. (*B*) The length distribution of the unlabeled actin is measured after 3 h of polymerization and 50 h later after subsequent labeling with Alexa 488-phalloidin. No significant change is observed, suggesting that the system has reached steady state.

and treadmilling have qualitatively different effects on the length distribution of visible filaments, such an experiment should reveal the dominant process and thus provide new insights into the steady-state dynamics of an ensemble of actin filaments.

To visualize the dynamic processes, we mix labeled filaments with a 300-fold excess of unlabeled filaments after 3 h of polymerization. The sample is split such that for each observation a new aliquot can be used to measure the length distribution of visible filaments $D_{\mathrm{vis}}(x)$ (Fig. 1 *A*). This procedure guarantees the avoidance of any artifacts by bleaching and filament fragmentation induced by the observation process. Directly before observations are made, the actin is stabilized with unlabeled phalloidin.

Fig. 2 shows typical fluorescence images taken during the experiment. It is clear that the length of the visible filaments decreases over time, indicating a dynamic exchange between the labeled and unlabeled filaments. Over the whole time course of the experiment, the complementary cumulative length distribution of visible filaments is well described by a single exponential, i.e., $D_{\mathrm{vis}}^{\mathrm{cum}}(x,t) = A_{\mathrm{vis}}^{\mathrm{cum}}(t)\cdot e^{-x/\lambda_{\mathrm{vis}}(t)}$ (Fig. 3 *A*). The decay length $\lambda_{\mathrm{vis}}(t)$ and thus the average visible filament length significantly decrease over time (Fig. 3 *C*). The initial decay length is found to be $\lambda_{\mathrm{vis}} \approx 4.3\ \mu$m, and it decreases to $\lambda_{\mathrm{vis}} \approx 1.1\ \mu$m after 52 h. This corresponds to an increase of the prefactor of the noncumulative length distribution $A_{\mathrm{vis}}(t) = A_{\mathrm{vis}}^{\mathrm{cum}}(t)/\lambda_{\mathrm{vis}}(t)$ over time (Fig. 3 *D*).

This finding is in sharp contrast to what would be expected if treadmilling were the dominant process. For the rather long filaments observed in our assay, the turnover rate and the diffusive length fluctuations can be expected to be independent of the filament length. Consequently, the length distribution would be uniformly shifted to shortened filaments, which is manifested in a decrease of the prefactor $A_{\mathrm{vis}}(t)$ but a constant decay length $\lambda_{\mathrm{vis}}(t)$. Thus, the observation of a decreasing decay length $\lambda_{\mathrm{vis}}(t)$ demonstrates that a major process has to depend on the filament length. One such process is spontaneous fragmentation.

In the simplest model, spontaneous fragmentation occurs with the same probability at any site between actin protomers (18). This results directly in a linear dependence of the filament fragmentation rate on the filament length. Because filaments consist of many subunits, we can describe them as continuous objects, breaking at random positions with the rate $k_0\mathrm{d}x$. Neglecting in a first approximation the association and dissociation of monomers, the length distribution of the visible parts of filaments $D_{\mathrm{vis}}(x,\ t)$ can be described by the following master equation:

$$\partial_t D_{\mathrm{vis}}(x,t) \;=\; -k_0 x D_{\mathrm{vis}}(x,t) + 2k_0 \int_x^\infty dx' D_{\mathrm{vis}}(x',t). \qquad (1)$$

The first term describes that a visible segment with length $x$ vanishes when it breaks with rate $k_0 x$. The second term describes that additional visible segments with length $x$ are created when longer filaments with length $x' > x$ break into two fragments. With the initial exponential distribution $D_{\mathrm{vis}}(x, t=0) = A_0 e^{-x/\lambda_0}$, the solution of this equation is given by

$$D_{\mathrm{vis}}(x,t) \;=\; A_0\cdot(1+k_0\lambda_0 t)^2\cdot e^{\dfrac{-x(1+k_0\lambda_0 t)}{\lambda_0}}. \qquad (2)$$

The reverse process (filament annealing) does not have to be accounted for, because there is a 300-fold excess of unlabeled filaments, and thus annealing events between two labeled filaments are extremely rare. Moreover, in the fragmentation model used here, the total length of the filaments, including invisible parts, does not play a role in the fragmentation rate of the labeled parts. Indeed, the observed decrease of the decay length $\lambda_{\mathrm{vis}}(t)$, which is not affected by length-independent processes (not accounted for here), can be fitted by this fragmentation model (Fig. 3 *C*). The resulting local rate of spontaneous fragmentation $k_0 = 6.4 \times 10^{-3}\ \mathrm{h}^{-1}\mu\mathrm{m}^{-1}$, corresponding to $k_0 = 4.8 \times 10^{-9}\mathrm{s}^{-1}$ per F-actin protomer, is surprisingly similar to the value of $k_0 = 1 \times 10^{-8}\mathrm{s}^{-1}$ as estimated by Erickson (19) from polymerization experiments performed by Wegner (18) at higher salt concentrations and higher temperature than used in this study. Very similar values were also suggested by other studies (20,27). Using the values obtained for $k_0$ and $\lambda_0 = 4.2\ \mu$m from the fit of $\lambda_{\mathrm{vis}}(t)$, and setting $A_0 = 29$ a.u. to calculate the expected time evolution of $A_{\mathrm{vis}}(t)$, we find that the model overestimates the increase of $A_{\mathrm{vis}}(t)$ (Fig. 3 *D*). This overestimation can be rationalized by the fact that treadmilling and diffusive

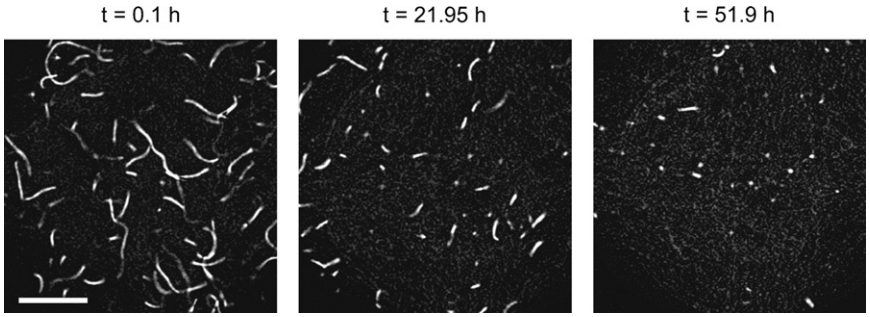


FIGURE 2 Typical fluorescence images (background subtracted, brightness adjusted) of labeled actin filaments mixed with unlabeled filaments are shown for three points of time during the experiment shown in Fig. 3 *A*. Each time, a new aliquot of the sample is used to avoid artifacts due to observation. Clearly, the lengths of the visible filaments decrease over time. Scale bar denotes 20 $\mu$m.

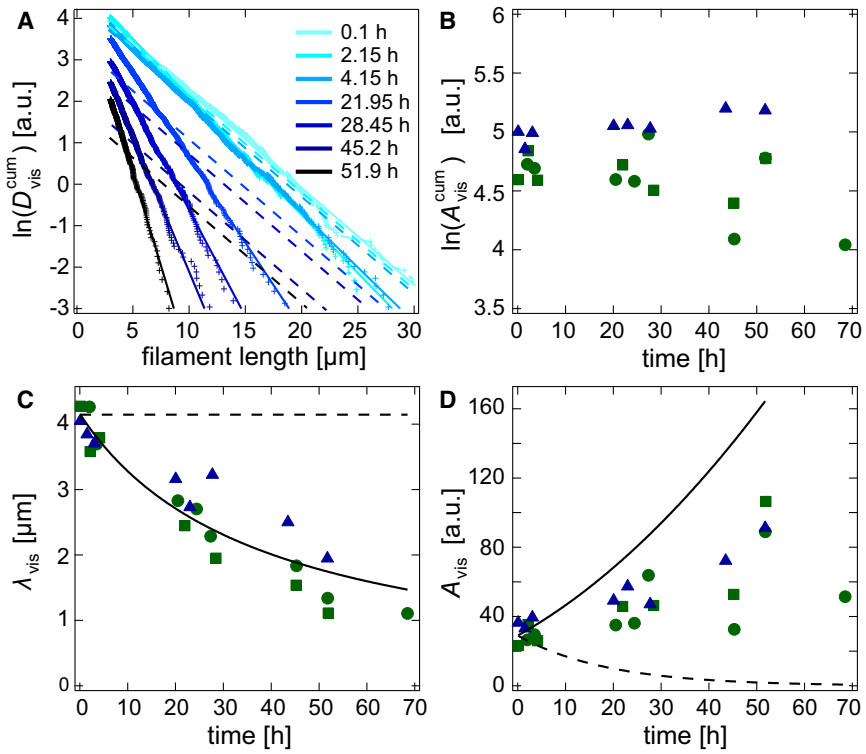


FIGURE 3 (*A*) Time evolution of the complementary cumulative length distribution $D_{\mathrm{vis}}^{\mathrm{cum}}(x, t)$ of Alexa Fluor 555-labeled actin filaments (33 nM) in an unlabeled F-actin solution (10 $\mu$M). Solid lines show exponential fits $D_{\mathrm{vis}}^{cum}(x,t) = A_{\mathrm{vis}}^{cum}(t)e^{-x/\lambda_{\mathrm{vis}}(t)}$. Dashed lines show the evolution of the initial exponential distribution as expected if just treadmilling with a turnover rate of 0.23 $\mu$m/h is considered. (*B–D*) The natural logarithm of the prefactor $A_{\mathrm{all}}^{\mathrm{cum}}(t)$ (*B*) and the decay length $\lambda_{\mathrm{vis}}(t)$ (*C*) of the exponential fit functions to the complementary cumulative length distributions, as well as the prefactor of the noncumulative length distribution $A_{\mathrm{vis}}(t) = A_{\mathrm{all}}^{\mathrm{cum}}(t)/\lambda_{\mathrm{vis}}(t)$ (*D*), are shown as a function of time for three independent experiments, where actin has been labeled with Alexa Fluor 555 (*green squares and circles*) or Atto 488 (*blue triangles*). Solid lines in *C* and *D* show a simple fragmentation model assuming a local fragmentation rate $k_0$ that is independent of the position in the filament and the filament length (Eq. 2). The value of $k_0 = 6.4 \times 10^{-3}\,\mathrm{h}^{-1}\mu\mathrm{m}^{-1}$ is obtained from a best fit to $\lambda_{\mathrm{vis}}(t)$ (*C*). Dashed lines show the time evolution as expected if just treadmilling with a turnover rate of $\mu$m/h is considered.

length fluctuations have been neglected. These processes result in a decrease of $A_{\mathrm{vis}}(t)$ as long as the ends of the labeled filaments have not annealed with unlabeled filaments. On the other hand, the deviation may also indicate that the local fragmentation rate is not completely independent of the filament length, resulting in nonlinear fragmentation and annealing rates.

To determine whether fragmentation is indeed the dominant process accounting for the dynamics of an F-actin solution, it is useful to obtain an independent estimate of the turnover rate. However, it is difficult to calculate the turnover rate from literature values because the association and dissociation rates for ATP, ADP-Pi, and ADP-actin at the barbed and pointed ends have to be known. In addition, most literature values were obtained from polymerization experiments and thus may differ from steady-state rates (15). Therefore, a direct measurement of the turnover rate would be preferable. Protomers involved in treadmilling eventually release their bound $\gamma$-phosphate (28). Thus, we can estimate an upper bound for the turnover rate of actin filaments by measuring the phosphate release of the system. To exclude the possibility that labeling significantly alters the rate of ATP hydrolysis, we investigated both of the fluorescently labeled actins used in this study (Alexa Fluor 555-labeled actin and Atto 488-labeled actin) in addition to unlabeled actin. As shown in Fig. 4 *A*, for 10 $\mu$M actin, phosphate is released at rates between 0.54 $\mu$M/h and 0.92 $\mu$M/h. The difference of the values obtained for different types of actin is not larger than the difference between two independent measurements of the same type of actin. Thus, within the experimental error, labeling has no influence on the rate of ATP hydrolysis. From the measured phosphate release rate, it can be estimated that most G-actin molecules have bound ATP. ADP-actin is expected to exchange its nucleotide to ATP on the timescale of minutes (29). Because the critical concentration is on the order of 1 $\mu$M (6), and $<1$ $\mu$M phosphate is released per hour, the nucleotide exchange can be expected to be fast enough to guarantee that most G-actin molecules have bound ATP.

To calculate the ATP hydrolysis rate per filament, we have to determine the total number of actin filaments from the length distribution of filaments and the F-actin concentration. Here, the length distribution of the unlabeled actin used for the phosphate assay is determined with fluorescence microscopy after labeling with Alexa 488-phalloidin (Invitrogen; Fig. 4 *B*), and a distribution similar to that shown in Fig. 1 *B* is found. If this exponential length distribution $D_{\mathrm{all}}(x) = A_{\mathrm{all}} \cdot e^{-x/\lambda_{\mathrm{all}}}$ with $\lambda_{\mathrm{all}} = 5.4$ $\mu$m is assumed to be valid also at filament lengths shorter than 3 $\mu$m, the concentration of filaments can be calculated to be $n_{\mathrm{all}} = \int D_{\mathrm{all}}(x)dx = A_{\mathrm{all}} \cdot \lambda_{\mathrm{all}}$. Because the critical concentration is small compared with the total actin concentration, the total length of actin filaments is given by the overall actin concentration times the length per protomer, $\int x \cdot D_{\mathrm{all}}(x)dx = A_{\mathrm{all}} \cdot \lambda_{\mathrm{all}}^2 = 10\ \mu\mathrm{M} \cdot 2.7\mathrm{nm}$, the prefactor $A_{\mathrm{all}}$ can be determined and a filament concentration of $n_{\mathrm{all}} =$ 5 nM results. Because 10 $\mu$M of actin hydrolyze 0.89 $\mu$M of

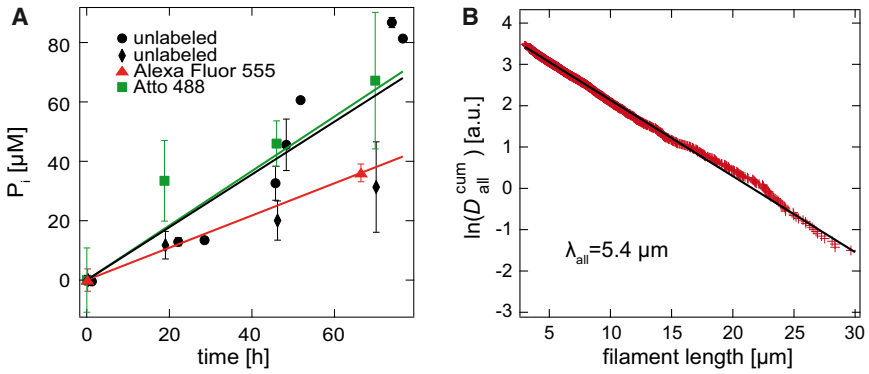


FIGURE 4 (*A*) Concentration of phosphate released by 10 $\mu$M steady-state F-actin shown as a function of time. Two independent series of measurements are performed for unlabeled actin (*black circles* and *diamonds*). Actin labeled with Alexa Fluor 555 (*red triangles*) or Atto 488 (*green squares*) is tested to exclude labeling artifacts. Error bars show the standard deviation for one to six data points measured at the respective points of time. Solid lines show fits assuming constant phosphate release rates for each type of actin. The two series of experiments with unlabeled actin are fitted globally and a rate of 0.89 $\mu$M/h is obtained. Rates of 0.54 $\mu$M/h and 0.92 $\mu$M/h are obtained for Alexa Fluor 555-labeled actin and Atto 488-labeled actin, respectively. (*B*) To correlate the measured phosphate release rate with a turnover rate, we need to determine the total number of F-actin filaments. For this purpose, unlabeled F-actin is polymerized and subsequently labeled with Alexa 488-phalloidin, and the complementary cumulative length distribution is measured. To minimize the experimental error due to variations between different actin preparations, we use the same actin preparation employed for one of the phosphate release measurements shown in panel *A* (*black circles*) to measure the length distribution of actin filaments.

ATP per hour (Fig. 4), the upper bound for the turnover rate is 0.48 $\mu$m/h, which corresponds to 0.05 protomers per second. From analogous calculations using the respective initial decay lengths of the measurements shown in Fig. 3, we obtain upper bounds for the turnover rates of 0.23 $\mu$m/h for Alexa Fluor 555-labeled actin and 0.37 $\mu$m/h for Atto 488-labeled actin. Using the turnover rate obtained for Alexa Fluor 555-labeled actin, we can calculate the change of the length distribution of visible filaments in an unlabeled network that would be expected if only treadmilling occurs: The exponential fit function of the initial distribution is simply shifted by 0.23 $\mu$m/h $\times$ $t$ (*dashed lines* in Fig. 3 *A*). As shown in Fig. 3, *C* and *D*, $\lambda_{vis}(t)$ would stay constant while $A_{vis}(t)$ would decrease exponentially. Still, the expected effect is on the same order of magnitude as the observed changes attributed to spontaneous fragmentation. Thus, treadmilling could significantly contribute to the time evolution of the labeled filaments, and thus could account for the deviation of the observed increase of $A_{vis}(t)$ over time from what is expected from our fragmentation model.

The assumption of a single exponential length distribution even for short filament lengths (<3 $\mu$m) is not indisputable. The double exponential decay of depolymerization curves measured with a pyrene assay has been suggested to indicate a double exponential length distribution (24,30). A higher number of short filaments than expected from a single exponential length distribution would result in an underestimation of the filament concentration and thus an overestimation of the turnover rate. Nevertheless, a lower treadmilling rate would also be consistent with the result that spontaneous fragmentation is a crucial process in the dynamics of a steady-state F-actin solution. However, in this case, other processes have to account for the fact that $A_{vis}(t)$ increases more slowly than expected from spontaneous fragmentation with a constant local rate of fragmentation.

## CONCLUSION

By following the length distribution of labeled actin filaments in an unlabeled F-actin solution, we were able to separate processes that cause shrinkage of filaments from growth processes that balance this shrinkage during steady state. In this study, we used a low-salt polymerization buffer because preliminary experiments with buffers containing additional KCl showed a drastic slowdown of actin dynamics compared with the low-salt buffer (see Supporting Material), as expected from the work of Pardee et al. (8). A change in the length distribution of labeled actin filaments in an unlabeled F-actin solution is hardly resolvable at the more-physiological buffer conditions, where thus both treadmilling and spontaneous fragmentation can be expected to occur at slower rates. We have shown that, at low salt conditions, treadmilling and diffusive length fluctuations do not dominate the shrinkage of labeled filaments in an unlabeled F-actin solution. In fact, only processes that depend on filament length—most probably spontaneous fragmentation—can account for the observed decrease in the decay length of the exponential length distribution of visible filaments. Assuming that filaments break with the same probability at any site between actin protomers, we determined the fragmentation rate to be $k_0 = 4.8 \times 10^{-9}\text{s}^{-1}$ per F-actin protomer. Because the dynamics of steady-state actin are even slowed down at more-physiological salt conditions, it can be expected that spontaneous fragmentation does not play a direct role in in vivo processes. However, in similarity to treadmilling, regulatory proteins can shift the rate of fragmentation to a faster timescale such that it becomes relevant for cytoskeletal processes (22,31).

Although the assay used in this study is perfectly suited to gain information about the overall behavior of an ensemble of actin filaments, also in the presence of regulatory proteins, and can be used to test theoretical models, other techniques will be needed to unambiguously identify the underlying microscopic processes.

## SUPPORTING MATERIAL

A figure is available at http://www.biophysj.org/biophysj/supplemental/S0006-3495(11)00838-1.

We thank M. Rusp for the actin preparation and S. Koehler for actin labeling.

We gratefully acknowledge funding from the European Research Council under the European Union's Seventh Framework Programme (FP7/2007-2013)/ERC CompNet (279476). K.M.S. acknowledges support from CompInt in the framework of the Elite Network of Bavaria Bayern and the International Graduate School of Science and Engineering. T.N. thanks Reinhard Lipowsky for support. A.R.B. acknowledges the great hospitality of the Kavli Institute for Theoretical Physics (National Science Foundation grant No. PHY05-51164) during the final stages of the manuscript writing.

## REFERENCES

1. Carlier, M. F., and D. Pantaloni. 2007. Control of actin assembly dynamics in cell motility. *J. Biol. Chem.* 282:23005–23009.
2. Loisel, T. P., R. Boujemaa, …, M. F. Carlier. 1999. Reconstitution of actin-based motility of *Listeria* and *Shigella* using pure proteins. *Nature*. 401:613–616.
3. Bernheim-Groswasser, A., S. Wiesner, …, C. Sykes. 2002. The dynamics of actin-based motility depend on surface parameters. *Nature*. 417:308–311.
4. Wegner, A. 1976. Head to tail polymerization of actin. *J. Mol. Biol.* 108:139–150.
5. Pollard, T. D., and M. S. Mooseker. 1981. Direct measurement of actin polymerization rate constants by electron microscopy of actin filaments nucleated by isolated microvillus cores. *J. Cell Biol.* 88:654–659.
6. Pollard, T. D. 1986. Rate constants for the reactions of ATP- and ADP-actin with the ends of actin filaments. *J. Cell Biol.* 103:2747–2754.
7. Wegner, A., and J.-M. Neuhaus. 1981. Requirement of divalent cations for fast exchange of actin monomers and actin filament subunits. *J. Mol. Biol.* 153:681–693.
8. Pardee, J. D., P. A. Simpson, …, J. A. Spudich. 1982. Actin filaments undergo limited subunit exchange in physiological salt conditions. *J. Cell Biol.* 94:316–324.
9. Simpson, P. A., and J. A. Spudich. 1980. ATP-driven steady-state exchange of monomeric and filamentous actin from Dictyostelium discoideum. *Proc. Natl. Acad. Sci. USA*. 77:4610–4613.
10. Asakura, S., and F. Oosawa. 1960. Dephosphorylation of adenosine triphosphate in actin solutions at low concentrations of magnesium. *Arch. Biochem. Biophys.* 87:273–280.
11. Korn, E. D., M.-F. Carlier, and D. Pantaloni. 1987. Actin polymerization and ATP hydrolysis. *Science.* 238:638–644.
12. Fujiwara, I., S. Takahashi, …, S. Ishiwata. 2002. Microscopic analysis of polymerization dynamics with individual actin filaments. *Nat. Cell Biol.* 4:666–673.
13. Kuhn, J. R., and T. D. Pollard. 2005. Real-time measurements of actin filament polymerization by total internal reflection fluorescence microscopy. *Biophys. J.* 88:1387–1402.
14. Fujiwara, I., D. Vavylonis, and T. D. Pollard. 2007. Polymerization kinetics of ADP- and ADP-Pi-actin determined by fluorescence microscopy. *Proc. Natl. Acad. Sci. USA*. 104:8827–8832.
15. Kueh, H. Y., W. M. Brieher, and T. J. Mitchison. 2008. Dynamic stabilization of actin filaments. *Proc. Natl. Acad. Sci. USA*. 105:16531–16536.
16. Kueh, H. Y., and T. J. Mitchison. 2009. Structural plasticity in actin and tubulin polymer dynamics. *Science.* 325:960–963.
17. Bugyi, B., and M.-F. Carlier. 2010. Control of actin filament treadmilling in cell motility. *Annu Rev Biophys.* 39:449–470.
18. Wegner, A. 1982. Spontaneous fragmentation of actin filaments in physiological conditions. *Nature.* 296:266–267.
19. Erickson, H. P. 1989. Co-operativity in protein-protein association. The structure and stability of the actin filament. *J. Mol. Biol.* 206:465–474.
20. Sept, D., J. Xu, …, J. A. McCammon. 1999. Annealing accounts for the length of actin filaments formed by spontaneous polymerization. *Biophys. J.* 77:2911–2919.
21. Fass, J., C. Pak, …, A. Mogilner. 2008. Stochastic simulation of actin dynamics reveals the role of annealing and fragmentation. *J. Theor. Biol.* 252:173–183.
22. Berro, J., V. Sirotkin, and T. D. Pollard. 2010. Mathematical modeling of endocytic actin patch kinetics in fission yeast: disassembly requires release of actin filament fragments. *Mol. Biol. Cell.* 21:2905–2915.
23. Spudich, J. A., and S. Watt. 1971. The regulation of rabbit skeletal muscle contraction. I. Biochemical studies of the interaction of the tropomyosin-troponin complex with actin and the proteolytic fragments of myosin. *J. Biol. Chem.* 246:4866–4871.
24. Schmoller, K. M., C. Semmrich, and A. R. Bausch. 2011. Slow down of actin depolymerization by cross-linking molecules. *J. Struct. Biol.* 173:350–357.
25. Webb, M. R. 1992. A continuous spectrophotometric assay for inorganic phosphate and for measuring phosphate release kinetics in biological systems. *Proc. Natl. Acad. Sci. USA*. 89:4884–4887.
26. Kawamura, M., and K. Maruyama. 1970. Electron microscopic particle length of F-actin polymerized in vitro. *J. Biochem.* 67:437–457.
27. Kinosian, H. J., L. A. Selden, …, L. C. Gershman. 1993. Actin filament annealing in the presence of ATP and phalloidin. *Biochemistry.* 32:12353–12357.
28. Melki, R., S. Fievez, and M. F. Carlier. 1996. Continuous monitoring of Pi release following nucleotide hydrolysis in actin or tubulin assembly using 2-amino-6-mercapto-7-methylpurine ribonucleoside and purine-nucleoside phosphorylase as an enzyme-linked assay. *Biochemistry.* 35:12038–12045.
29. Kinosian, H. J., L. A. Selden, …, L. C. Gersham. 1993. Nuceotide binding to actin. Cation dependence of nucleotide dissociation and exchange rates. *J. Biol. Chem.* 268:8683–8691.
30. Wendel, H., and P. Dancker. 1986. Kinetics of actin depolymerization: influence of ions, temperature, age of F-actin, cytochalasin B and phalloidin. *Biochim. Biophys. Acta.* 873:387–396.
31. Staiger, C. J., M. B. Sheahan, …, L. Blanchoin. 2009. Actin filament dynamics are dominated by rapid growth and severing activity in the *Arabidopsis* cortical array. *J. Cell Biol.* 184:269–280.